RSC Advances

ROYAL SOCIETY OF CHEMISTRY

www.rsc.org/advances

In-situ graft copolymerization of L-lactide onto cellulose and the melt direct spinning

Yue Zhang Xinda Li Yanping Yang Ai Lan Xiaoyun He and Muhuo Yu*

State Key Laboratory for Modification of Chemical Fibers and Polymer Materials,
College of Materials Science and Engineering,
Donghua University,
2999 North Renmin Road, Songjiang District, Shanghai 201620, China
* To whom correspondence should be addressed: (Tel: +86-21-67792887, Fax: +86-21-67792892, Email: yumuhuo@dhu.edu.cn)

Abstract: In order to prepare bio-degradable cellulose-based fibers in an environmentally-friendly way, graft copolymerization of L-lactide (LLA) onto cellulose was carried out through a co-rotating twin-screw extruder and then the blend melt was directly spun. Ionic liquid namely 1-allyl-3-methylimidazolium chloride ([AMIM]Cl) was used as reaction medium and tin(II) octoate was used as catalyst. The graft copolymerization effect was evaluated by the study of FTIR, ^{13}C-NMR, WAXD, TGA and SEM. The results indicated that LLA successfully in-situ grafted onto the cellulose backbone and PLA long-chain branches were formed, which restrained the thermal and photo degradation of regenerated cellulose and hindered the crystallization of cellulose. The morphology of cellulose-graft-polylactide blend fiber showed smooth surface and ductile cross section due to the destruction of hydrogen bond network of cellulose and the better thermoplastic of PLA branches. Because cellulose-g-PLA blend with 1000 g LLA prepared at 50 rpm rotation speed has good spinnability, drawability and thermostability, the mechanical properties of this fiber were better than other cellulose-g-PLA blend fibers. Compare to other commercial cellulose fibers, the in-situ graft copolymerization modification of cellulose with LLA resulted in better mechanical properties of cellulose-based fibers, high efficiency of cellulose fiber production and less energy consumption of solvent recycle.

Keywords: cellulose; polylactide; ionic liquids; in-situ graft copolymerization; extrusion.

1. Introduction

With increased awareness of the environmental protection and the increased price of crude oil, environmental issues connected to white pollution caused by petroleum based materials attracted increasing attention, which has driven more scientific research into the development of renewable biomass materials such as cellulose and polylactide (PLA).[1-2] For example, many researches focus on the development of a new range of cellulose/PLA biodegradable composite materials.[3-6] However, cellulose cannot be processed by melt-extrusion or melt-spinning like thermoplastic because of the strong hydrogen-bonding interactions and high crystallinity, so cellulose is commonly used as filler in the cellulose/PLA composites. Unfortunately, most natural polymers like cellulose are hydrophilic materials since they contain hydroxyl groups, while most synthetic biodegradable polymers, especially the aliphatic polyesters like PLA, are hydrophobic. Therefore, cellulose and PLA are thermodynamically immiscible and thus, compatibility problems must be solved first in order to obtain competitive materials. In recent years, researches on the chemical grafting of cellulose with L-lactide (LLA) have been attracting more and more scientists and the results indicated the potential applicability of cellulose-graft-polylactide (cellulose-g-PLA) in drug delivery system, personal care products and packaging industry. [7-11]

Due to the presence of three hydroxyl groups in each glucose residue, cellulose is only soluble in particular solvents such as NaOH/CS_2, N-methyl morpholine oxide (NMMO), NaOH/urea aqueous solution and ionic liquid (IL),[12-16] but the dissolubility of cellulose in these solvents is only 5-15 % with heating and stirring for 2-4 h. The massive solvent and long-time dissolution may cause serious degradation of cellulose and decrease the production efficiency of cellulose fibers,[17-18] which limited the industry development and application of cellulose-g-PLA copolymer in the fiber field.

In order to decrease the intermolecular force of cellulose in a green and high

efficient way, the graft copolymerization of cellulose with LLA was conducted in a continuous reactor co-rotating twin screw extruder in this paper. 1-allyl-3-methylimidazolium chloride ([AMIM]Cl) was used as reaction medium. Cl^- from [AMIM]Cl can act as small hydrogen bond acceptor to interrupt the extensive intermolecular and intramolecular hydrogen bonding of cellulose.[19-20] Tin (II) octoate ($Sn(Oct)_2$) was used as catalyst. Sn^{2+} can abstract protons from the hydroxyl groups of cellulose to facilitate graft copolymerization.[21-22] Under the shearing and conveying of twin-screw, cellulose will be well crushed, plasticized in [AMIM]Cl, blended with LLA and grafted with PLA. We attempt to introduce PLA flexible side chain at cellulose backbone during extrusion to reserve the biodegradability of cellulose and even realize the melt-spinning of cellulose. At the same time, the low-melt viscosity and low-heat distortion temperature of PLA can be improved by copolymerization.

To the best of our knowledge, the graft copolymerization modification of cellulose was only conducted in the batch reactor so far and no report has been published on the in-situ graft copolymerization of cellulose through reactive extrusion as well as the production of cellulose-based fibers by melt direct spinning.[23-24] Owing to the high shear stress of twin-screw extruder, the reaction time and the amount of solvent used in this paper are both far less than those used in other published literatures. The implementation of this work will provide theory directions to the development of cellulose's melt spinning and improve the environment, production efficiency and fiber properties.

2. Experimental

2.1 Materials

Cotton cellulose was supplied by Jiangsu Longma green fiber industry Co., Ltd. DP = 550. [AMIM]Cl was purchased from Shanghai Chengjie Chemical industry Co., Ltd. T_m = 73.0 ^oC. Tin(II) octoate ($Sn(Oct)_2$) was from Sinopharm Chemical Reagent Co., Ltd. L-lactide (LLA) was purchased from Purac, T_m = 93 ^oC. Alcohol (AR) and chloroform (AR) were came from Shanghai Jingchun industry Co., Ltd.

2.2 Methods

Cellulose powder was dried under vacuum at 70 ^oC for 24 h. With 600 g of

[AMIM]Cl as reaction medium and 5, 10 or 15 g of ($Sn(Oct)_2$) as catalyst, 200 g of cellulose was in-situ graft copolymerized with 500, 1000 or 1500 g of LLA by reactive extrusion in a co-rotating twin-screw extruder (L/D = 48, D = 35 mm), respectively. The barrel temperatures of the extruder from zone 1 to zone 9 were 100, 110, 120, 120, 130, 130, 140, 140 and 150 ^{o}C. The screw rotation speed was 50 rpm. The spinning temperature was 160 ^{o}C. The winding speed was 500 m/min. After spinning, the fiber was washed several times with distilled water and alcohol successively to remove [AMIM]Cl and unreacted LLA, then dried at 60 ^{o}C for 24 h in a vacuum oven. Besides, the mixture of cellulose/[AMIM]Cl (200 g/600 g) was also spun and purified at the same condition, named as regenerated cellulose.

2.3 Characterizations

Fourier-transform infrared (FTIR) spectroscopy with an attenuated total reflectance (ATR) accessory was performed on a Nicolet Nexus 670 + Raman Module (Thermo Fisher, America). The scan of each sample was recorded from 4000 to 400 cm^{-1} at a resolution of 2 cm^{-1} in the transmission mode.

Cross-Polarisation Magic Angle Spinning Carbon-13 solid-state Nuclear Magnetic Resonance spectra (CP/MAS ^{13}C-NMR) was performed on Bruker DSX-400 spectrometer (Karlsruhe, Germany) under a static field strength of 2.3 T at 25 ^{o}C. The contact time for CP was 1 ms with a proton pulse of 5.5 ms and decoupling power of 45 kHz. The MAS speed was 3 kHz and the delay time after the acquisition of the FID signal was 2 s.

Wide-angle X-ray diffraction (WAXD) measurements were carried out with D/max 2250VB/PC X-ray diffractometer with Cu/Kα_1 radiation (Rigaku, Japan). Diffraction patterns of samples were obtained in the reflection mode from 3 to 50 ^{o} of 2θ at a scanning speed of 0.02 ^{o}/s.

Before FTIR, ^{13}C-NMR and WAXD tests, cellulose-g-PLA blend fiber were extracted by chloroform in a Soxhlet extractor for 24 h to remove PLA homopolymer.

Steady-state rheological measurements were performed with a HAAKE RS150L Rheometer (USA), equipped with cone-plate geometry. The experiments were performed at 160 ^{o}C with a shear rate (γ) range of 0.1 to 450 s^{-1} under a nitrogen

atmosphere.

Thermalgravimetric analysis (TGA) was performed using a simultaneous thermal analyzer (Netzsch TG209F1). The samples mass varied between 5 and 10 mg. Temperature programs for dynamic tests were run from 50 to 600 ^{o}C at heating rates of 5 ^{o}C/min in air atmosphere.

Ultraviolet photo degradation tests were performed using ultraviolet ageing oven (Uvitron, America). The radiation intensity was 40 mW/cm^2. All measurements were performed at a temperature of 80 ^{o}C for 1-2 h.

The cross section and surface image of cellulose fibers were revealed by a JSM 6100 scanning electron microscopy (SEM).

Single fiber tensile properties were tested by XQ-1A Fiber Tensile Tester at a gauge of 10 mm. The sample length was 20 mm. The crosshead speeds used was 10 mm/min. All measurements were performed at a temperature of 20 ^{o}C and 65 % relative humidity. The results came from more than 25 measurements of each specimen.

3. Results and Discussions

3.1 Molecular structure

Figure 1 shows the FTIR spectra for original cellulose, regenerated cellulose and cellulose-g-PLA. As seen in Figure 1 (a) and (b), the band at the range of 3600-3000 cm^{-1} is related to the absorption of hydrogen-bonded hydroxyl groups and the band in the region of 2920-2850 cm^{-1} is assigned to the C-H stretching vibrations of cellulose. A strong band appeared at 1750 cm^{-1} in Figure 1 (c), which is related to the absorption of C=O stretching vibration. It proves that the graft copolymerization of cellulose with LLA indeed occurred and PLA side chains were in-situ synthesized on the cellulose backbone during reactive extrusion. The methyl asymmetric deformation of the branched LLA appears at 1460 cm^{-1}, and the symmetric C-O-C stretching vibrations of the ester group were also found around 1190 cm^{-1}. Moreover, a small new peak appears at 3000 cm^{-1} is ascribed to the stretching of CH_3 groups. It can be seen that the intensity of the peak at 3600-3000 cm^{-1} in regenerated cellulose are almost the same as that of original cellulose, indicating that the amount of [AMIM]Cl

added is not enough to destroy the hydrogen bonds of cellulose effectively. However, the intensity of the peak at 3600-3000 cm^{-1} in the cellulose-g-PLA reduced obviously, indicating that the intermolecular hydrogen bonds and intermolecular hydrogen bond are destructed effectively after reactive extrusion.

^{13}C-NMR spectra of pure cellulose, regenerated cellulose and cellulose-g-PLA are shown in Figure 2. Five major peaks were identified in the spectrum for pure cellulose, and the chemical shifts of carbon can be assigned to 104.5 ppm for C-1, 88.7 and 83.5 ppm for crystallized and amorphous C-4, 71.3 and 75.7 ppm for C-2, 3, 5 with nearly equal intensity, 65.3 and 62.2 ppm for crystallized and amorphous C-6. methyl carbon (CH_3) signals of PLA branches was observed as a doublet at 16.5 and 19.4 ppm, respectively. Moreover, a new peak appeared at about 169.4 ppm, which is related to the carbon chemical shifts of carbonyl group (C=O) for PLA, but the signals of methenyl group (C-H) of PLA at about 66 ppm was overlapped by the signals of amorphous C-6 carbon. The formation of long-chain branches of PLA restrained the self-association of cellulose molecules, leading to the retardation of cellulose crystallization. Therefore, the relative intensity ratio of crystallized C-4 signal/amorphous C-4 signal decreased obviously for the cellulose-g-PLA.

3.2 Crystal structure

The WAXD spectra of original cellulose, regenerated cellulose and cellulose-g-PLA were shown in Figure 3. The peaks appear at 14.8^o, 16.5^o, 22.7^o and 34.2^o in the diffraction pattern of original cellulose and regenerated cellulose correspond to the (101), ($10\bar{1}$), (002) and (040) crystal planes, respectively, which are the characteristic peaks of cellulose-I crystalline structure, indicating that the amount of [AMIM]Cl is not enough to enforce the crystalline transformation to cellulose-II. However, the diffraction pattern of cellulose-g-PLA copolymer shows the characteristic peaks of cellulose-II crystalline structure at 12.0^o, 19.7^o and 22.0^o, respectively and another diffraction peak appears at 16.0^o, corresponding to the (101) crystal plane of PLA. It indicated that LLA reacted with glucan chain hydroxyl groups to prevent fibrils from approaching one another, which resulted in the lattice

relaxation of cellulose. On the other hand, the formation of long-chain branches on the cellulose backbone destructed the structure regularity and orientation of cellulose and finally destructed the crystal structure of original cellulose seriously.

3.3 Spinnability

Rheological behaviour of cellulose/[AMIM]Cl and cellulose-g-PLA/[AMIM]Cl blends with different amount of LLA were measured at high temperature (160 ^{o}C) and high shear rate (0.1-450 s^{-1}) by cone plate rheometer. The structural viscosity index ($\Delta\eta$) is a useful experimental parameter for the spinnability of spinning dope. The $\Delta\eta$ can be obtained by the following equation:[25]

$$\Delta\eta = -d\lg\eta_a / d\gamma^{1/2} \times 100$$

where η_a is apparent viscosity and γ is shear rate.

The $lg\eta_a$ against $\gamma^{1/2}$ at 160 ^{o}C of cellulose/[AMIM]Cl and cellulose-g-PLA/[AMIM]Cl blends with different amount of LLA are given in Figure 4. LLA contents investigated varied from 2.5 to 7.5 times with respect to the weight of cellulose. The plots of $lg\eta_a$ vs. $\gamma^{1/2}$ for all the samples exhibit good linear relationship. The values of $\Delta\eta$ can be obtained from the slopes of the straight lines, as shown in Table 1. According to Table 1, the formation of PLA increased the degree of chain entanglement and restricted the segment slippage, so $\Delta\eta$ values of cellulose-g-PLA/[AMIM]Cl blends increased with the increase of LLA amount, especially when the content of LLA reached 1500g, $\Delta\eta$ values increase dramatically, indicating the flowability and spinnability of cellulose blends with 500-1000 g LLA are much better. The smaller $\Delta\eta$ values for the cellulose blends with 500-1000 g LLA can be attributed to the appropriate amount of long-chain branches in cellulose blends which disrupted hydrogen bonds of cellulose effectively. However, the molecules were tangled up seriously in cellulose blend with 1500 g LLA, resulting in a significant increase in the structured extent of the spinning melt. According to spinning experiments, the practical spinnability of cellulose/[AMIM]Cl and cellulose-g-PLA/[AMIM]Cl blends with different amount of LLA were summarized in Table 1. Due to the strong hydrogen bonding network of cellulose molecules, the

spinnability and flexibility of pure cellulose fiber were poor. It indicated that the amount of [AMIM]Cl is not enough to destroy the hydrogen bonds of cellulose completely. Through the creation of long-chain branches of PLA, the number of hydrogen groups of cellulose decreased and the distance between the cellulose molecules increased, so the melt flowability of cellulose-g-PLA blend with LLA 500g and LLA 1000g was improved obviously, but the cellulose-g-PLA blend with 1500g can be drawn only to 1.0 - 1.5 times its initial length. If drawn more, the blend fiber on the surface will crack and break, and the resulting fiber cannot withstand actual use.

3.4 Thermal stability

TGA and DTG curves for original cellulose, regenerated cellulose fiber and cellulose-g-PLA blend fiber are shown in Figure 5a and Figure 5b, respectively. Original cellulose powder presents one decomposition peak with maximum at 345.7 ^{o}C while DTG peak of the regenerated cellulose becomes wider and shifts to 286.3 ^{o}C. This is expected as the molecular chain of cellulose was interrupted after swelled or dissolved in [AMIM]Cl, so the polymerization degree and the thermal stability of regenerated cellulose was reduced. However, the cellulose-g-PLA presents two events. These events include the thermal decomposition of (1) PLA homopolymer, decomposed at 311.2 ^{o}C, which is mainly due to ester scission; (2) cellulose-g-PLA, decomposed at 361.6 ^{o}C, which is 15.9 ^{o}C higher than that of original cellulose. The formation of PLA long-chain branches on the backbone of cellulose disturbs the segment motion and causes the entanglement of cellulose chains, which counteracted the negative factors of [AMIM]Cl, so the thermal stability of cellulose-g-PLA blend fiber was improved effectively.

In order to investigate the effect of polymerization time - i.e. residence time on the fiber properties, the screw rotation speed increases from 25 rpm to 100 rpm. Figure 6 shows DTG curves of cellulose-g-PLA blend fiber prepared at different residence time. With the increase of screw rotation speed, the residence time decreased, so the weight loss of PLA homopolymer decreased obviously but the cellulose-g-PLA has critical point of decomposition temperature. It indicated that

when the screw rotation speed was 25 rpm, the graft copolymerization time between LLA and cellulose was long, but cellulose and PLA had a limited tolerance to shear rate and temperature, so cellulose and PLA degraded seriously with long-time heating and shearing. As shown in Figure 6 (a), the initial decomposition temperature of PLA homopolymer was only 226.6 ^{o}C and the peak decomposition temperature of cellulose-g-PLA shifted to 348.5 ^{o}C. On the whole, when the screw rotation speed was 50 rpm, cellulose-g-PLA blend fiber has better thermal stability.

3.5 Photo stability

The microscope pictures of regenerated cellulose fiber prepared by batch reactor, regenerated cellulose fiber prepared by twin-screw extruder and cellulose-g-PLA blend fiber after ultraviolet irradiation at 80 ^{o}C for 1-2 h were shown in Figure 7. During ultraviolet irradiation, hydroxyl groups on the C-2 and C-3 in each glucose residue of cellulose are most likely to be oxidized to form carbonyl compound which is the fundamental cause for cellulose turning yellow. Dissolution of cellulose in the batch reactor needs continuous heating and stirring for 2-4 h, leading to a serious degradation of cellulose, so the colour of fiber almost changed to brown, as shown in the Figure 7 (a). Compared to Figure 7 (b), the fiber for the 1 h irradiated in Figure 7 (c) was more yellowish, but after 2 h irradiated, the speed of colour change for the fiber in Figure 7 (c) was obviously slower. This may be because that the formation of PLA branches inhibit the orderly arrangement of cellulose chains and decreased the crystallizability of cellulose. At the initial stage of ultraviolet irradiation, cellulose chains broke first at the amorphous region, so cellulose-g-PLA blend fiber with more amorphous cellulose or imperfect crystallized cellulose turned yellow quickly. With the irradiation time extended, crystal region of cellulose begin to degrade, the long-chain branched structure may restrain photo degradation of cellulose-g-PLA blend fiber.

3.6 Morphology

SEM micrographs of regenerated cellulose fiber and cellulose-g-PLA blend fiber were displayed in Figure 8. As seen in Figure 8 (a) and (b), many flaws existed in the surface of regenerated cellulose fiber and the cross section was very rough. It

indicated that cellulose cannot be completely dissolved in [AMIM]Cl during extrusion when the weight ratio of [AMIM]Cl/cellulose is only 3, leading to the formation of partially dissolved cellulose and partially swollen cellulose. Therefore, the shrinkage between the cortex and core was different when the filaments of regenerated cellulose were cooled. However, cellulose-g-PLA blend fiber shows a smooth, uniform surface and flexible cross section. The formation of microfibrils can be observed in Figure 8 (d), which leads to better interfacial adhesion between cellulose and PLA and consequently finer distribution for the cellulose-g-PLA blend fiber. Owing to the high shear stress of twin-screw extruder, LLA can react with swollen or dissolved cellulose to in-situ form grafted copolymer cellulose-g-PLA. The PLA side chain can act as internal plasticizer to increase the mobility of cellulose and hence impart thermoplastic to cellulose.

3.7 Mechanical properties

The mechanical properties of modified cellulose fibers are shown in Table 2. Because cellulose-g-PLA blend with 1000 g LLA prepared at 50 rpm rotation speed has good spinnability, drawability and thermo stability, the mechanical properties of this fiber were better than other cellulose-g-PLA blend fibers. According to available reports, the breaking strength of viscose fiber and lyocell fiber is about 1.5-3.2 cN/dtex and 2.0-4.5 cN/dtex, respectively and the elongation at break of viscose fiber and lyocell fiber is about 15-25 % and 10-20 %, respectively.[26-28] Viscose fiber is the first commercial manmade fibers that was developed over 100 years ago, but the conventional viscose processes uses NaOH/CS_2 as solvents, leading to serious environmentally pollution. Lyocell fiber is commercialized by using NMMO/H_2O as a direct solvent which has been developed to reduce the processing steps as well as to minimize the hazardous byproducts in recent decades. However, the NMMO/H_2O system requires high temperature for dissolution and antioxidants to avoid side reactions of solvent, resulting in degradation of cellulose and high costs.[29-30] In this paper, the breaking strength of cellulose-g-PLA blend fiber is higher than that of viscose fiber and close to that of lyocell fiber. There were maybe two primary reasons: (1) the dissolubility of cellulose in NaOH/CS_2 is only 10-15 % with heating and

stirring for 2-4 h, but the dissolubility of cellulose in [AMIM]Cl is 33.3 % with twin-screw shearing for 10 min, so the short-time dissolution and little solvent avoided the degradation of cellulose, (2) the side chain of PLA in modified cellulose had better internal plasticization and stronger size exclusion effect. Moreover, the branched structure of cellulose-g-PLA promoted the chain entanglement and allowed much more chemical bond fracture in cellulose-g-PLA blend fiber, leading to a more efficient stress transfer under stress conditions and thereby better mechanical properties.

4. Conclusions

In this work, the in-situ graft copolymerization of cellulose-g-PLA by reactive extrusion and the direct melt spinning of extruded blends were investigated. FTIR and ^{13}C-NMR results proved that the grafting of LLA onto the backbone of cellulose was successfully achieved and the formation of PLA long-chain branches destructed hydrogen bond network of cellulose effectively. WAXD results revealed that the branch structure of cellulose-g-PLA copolymer disturbed the orientation of cellulose and realized cellulose I-II transition. TGA and photo degradation tests confirmed that PLA long-chain branches caused the chains entanglement and improved the thermal and photo stability of cellulose-g-PLA blend fiber. On the whole, as the content of LLA was 1000 g and the rotation speed was 50 rpm, the cellulose-g-PLA blend has better mechanical properties. The graft copolymerization with LLA improved the surface morphology of regenerated cellulose fiber and introduced plasticity to cellulose-based blend fiber, so breaking strength and elongation at break of the cellulose-g-PLA blend fiber were almost doubled in comparison with regenerated cellulose fiber.

Acknowledgements

Thanks for the financial assistance of Shanghai Yangfan Programm (14YF1405200) and Textile Vision Science & Education Fund of China.

References

[1] D. Klemm, B. Heublein, H. P. Fink and A. Bohn, Angew. Chem. Int. Ed., 2005, **44**, 3358.

[2] X. F. Niu, X. M. Li, H. F. Liu, G. Zhou, Q. L. Feng, F. Z. Cui and Y. B. Fan, J. Biomat. Sci-Polym. E., 2012, **23**, 391.

[3] L. Yu, K. Dean and L. Li, Prog. Polym. Sci., 2006, **31**, 576.

[4] R. Auras, B. Harte, S. Selke, Macromol. Biosci., 2004, **4**, 835.

[5] J. F. Zhang and X. Sun, J. Appl. Polym. Sci., 2004, **94**, 1697.

[6] R. L. Shogren, W. M. Doane, D. Garlotta, J. W. Lawton and J. L. Willett, Polym. Degrad. Stabil., 2003, **79**, 405.

[7] C. H. Yan, J. M. Zhang, Y. X. Lv, J. Yu, J. Wu, J. Zhang and J. S. He, Biomacromolecules, 2009, **10**, 2013.

[8] N. Lin, G. J. Chen, J. Huang, A. Dufresne and P. R. Chang, J. Appl. Polym. Sci., 2009, **113**, 3417.

[9] F. Quero, S. J. Eichhorn, M. Nogi, H. Yano, K. Y. Lee and A. Bismarck, J. Polym. Environ., 2012, **20**, 916.

[10] N. L. García, M. Lamanna, N. D'Accorso, A. Dufresne, M. Aranguren and S. Goyanes, Polym. Degrad. Stabil., 2012, **97**, 2021.

[11] H. Dong, Q. Xu, Y. Li, S. Mo, S. Cai and L. Liu, Colloid. Surface B., 2008, **66**, 26.

[12] H. Zhao, J. H. Kwak, Y. Wang, J. A. Franz, J. M. White and J. E. Holladay, Carbohydr. Polym., 2007, **67**, 97.

[13] B. Zhao, L. Greiner and W. Leitner, RSC Adv., 2012, **2**, 2476.

[14] W. Ronny, R. Stella and S. Anna, RSC Adv., 2012, **2**, 4472.

[15] Y. Zhang, X. D. Li, H. F. Li, M. E. Gibril, K. Q. Han and M. H. Yu, RSC Adv., 2013, **13**, 11732.

[16] K. Edgar, T. Heinze and T. Liebert, Cellulose solvents: for analysis, shaping and chemical modification, Washington DC: American Chemical Society, 2009.

[17] S. Barthel and T. Heinze, Green Chem., 2006, **8**, 301.

[18] R. P. Swatloski, S. K. Spear, J. D. Holbrey and R. D. Rogers, J. Am. Chem. Soc., 2002, **124**, 4974.

[19] Y. Zhang, H. F. Li, X. D. Li, M. E. Gibril and M. H. Yu, Carbohydr. Polym., 2014, **99**, 126.

[20] Y. Zhang, X. D. Li, H. F. Li, M. E. Gibril, K. Q. Han and M. H. Yu, J. Polym. Res., 2013, **20**, 171.

[21] J. Libiszowski, A. Kowalski, A. Duda and S. Penczek, Macromol. Chem. Phys., 2002, **203**, 1694.

[22] W. Z. Yuan, J. Y. Yuan, F. B. Zhang and X. M. Xie, Biomacromolecules, 2007, **8**, 1101.

[23] Y. H. Luan, J. Wu, M. S. Zhan, J. M. Zhang, J. Zhang, J. S. He, Cellulose, 2013, **20**, 327.

[24] T. Yoshikuni and N. Yoshiyuki, Polymer, 2003, **44**, 2701.

[25] P. Navard, J. M. Haudin, I. Quenin, A. Peguy. Shear rheology of diluted solutions of high molecular weight cellulose. J. Appl. Polym. Sci.,1986, **32**, 5829.

[26] R. Zhou, M. X. Yang. Research on Mechanical Properties of Several New Regenerated Cellulose Fibers. Advanced Materials Research. 2011, **332-334**, 489.

[27] H. P. Fink, J. Ganster, A. Lehmann. Progress in cellulose shaping: 20 years industrial case studies at Fraunhofer IAP. Cellulose, 2014, 21, 31.

[28] I. Shoaib, A, Zuhaib. Impact of degree or Polymerization of Fiber on Viscose Fiber Strength. Degree of Master in Textile Technology. The Swedish School of Textiles, 2011.

[29] H. Zhao, J. H. Kwak, Y. Wang, J. A. Franz, J. M. White, J. E. Holladay. Interactions between cellulose and N-Methylmorpholine-N-oxide. Carbohydrate Polymers. 2007, **67**, 97.

[30] L. Shen, M. K. Patel. Environmental impact assessment of man-made cellulose fibres, Netherlands: Utrecht University, 2010.

Table 1 Structural viscosity index of cellulose/[AMIM]Cl and cellulose-g-PLA /[AMIM]Cl blends

Samples	Δη	Spinnability
LLA 0 g	9.59	Brittle, discontinuous
LLA 500 g	11.66	Stable, continuous
LLA 1000 g	15.10	Stable, continuous
LLA 1500 g	21.21	Difficult to draw

Table 2 Mechanical properties comparison among regenerated cellulose fiber, cellulose-g-PLA blend fiber and other commercial cellulose fibers

Samples	Breaking strength (cN/dtex)	Elongation at break (%)
regenerated cellulose fiber	1.5	7.5
cellulose-g-PLA blend fiber (LLA500g 50rpm)	2.8	10.6
cellulose-g-PLA blend fiber (LLA1000g 50rpm)	4.1	13.4
cellulose-g-PLA blend fiber (LLA1000g 25rpm)	2.0	15.7
cellulose-g-PLA blend fiber (LLA1000g 75rpm)	3.7	12.2
cellulose-g-PLA blend fiber (LLA1000g 100rpm)	3.2	13.9
viscose fiber	1.5-3.2	15-25 %
lyocell fiber	2.0-4.5	10-20 %

Figure Captions

Figure 1 FTIR spectra of (a) original cellulose, (b) regenerated cellulose, (c) cellulose-g-PLA

Figure 2 ^{13}C-NMR spectra of (a) original cellulose, (b) regenerated cellulose, (c) cellulose-g-PLA

Figure 3 WAXD 2θ distributions of (a) original cellulose, (b) regenerated cellulose, (c) cellulose-g-PLA

Figure 4 $\lg\eta_a$ versus $\gamma_{1/2}$ for cellulose/[AMIM]Cl and cellulose-g-PLA/[AMIM]Cl blends

Figure 5 a TGA and **b** DTG curves of (a) original cellulose, (b) regenerated cellulose fiber, (c) cellulose-g-PLA blend fiber

Figure 6 DTG curves of cellulose-g-PLA blend fiber prepared at different screw rotation speed (a) 25 rpm, (b) 50 rpm, (c) 75 rpm, (d) 100 rpm

Figure 7 The microscope pictures of (a) regenerated cellulose fiber prepared by batch reactor, (b) regenerated cellulose fiber prepared by twin-screw extruder, (c) cellulose-g-PLA blend fiber after ultraviolet irradiation at 80 ^{o}C for 1-2 h

Figure 8 SEM morphologies of regenerated cellulose fiber: (a) surface, (b) cross section and cellulose-g-PLA blend fiber: (c) surface, (d) cross section

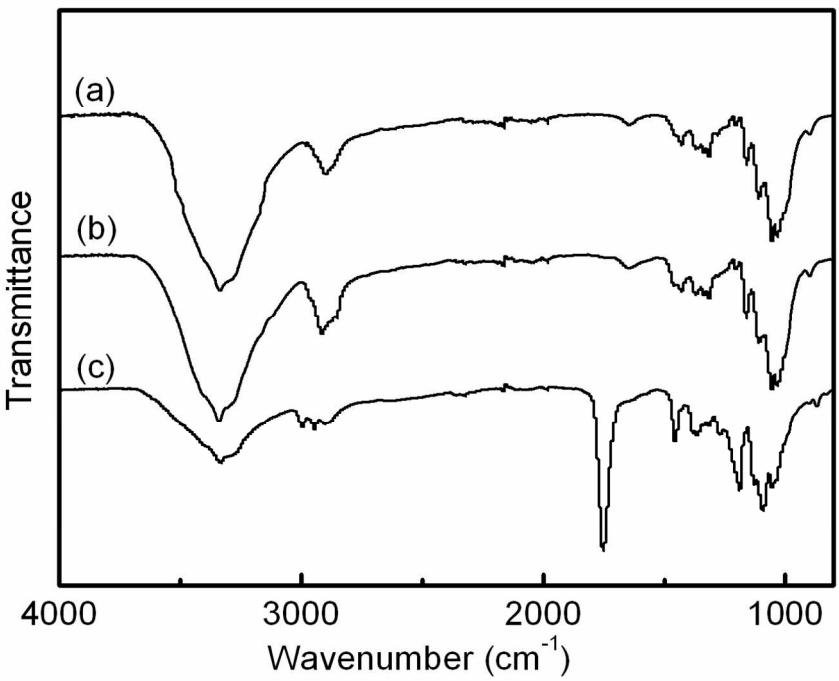

Figure 1 FTIR spectra of (a) original cellulose, (b) regenerated cellulose, (c) cellulose-g-PLA
261x219mm (150 x 150 DPI)

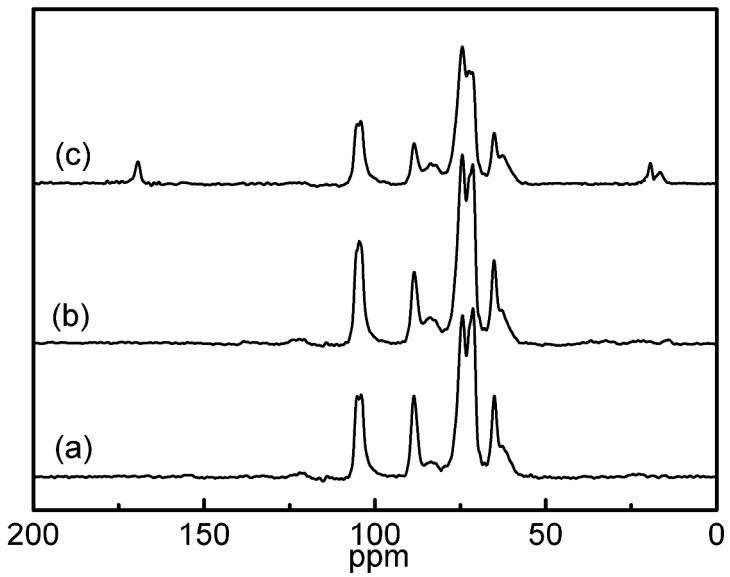

Figure 2 13C-NMR spectra of (a) original cellulose, (b) regenerated cellulose, (c) cellulose-g-PLA
289x202mm (300 x 300 DPI)

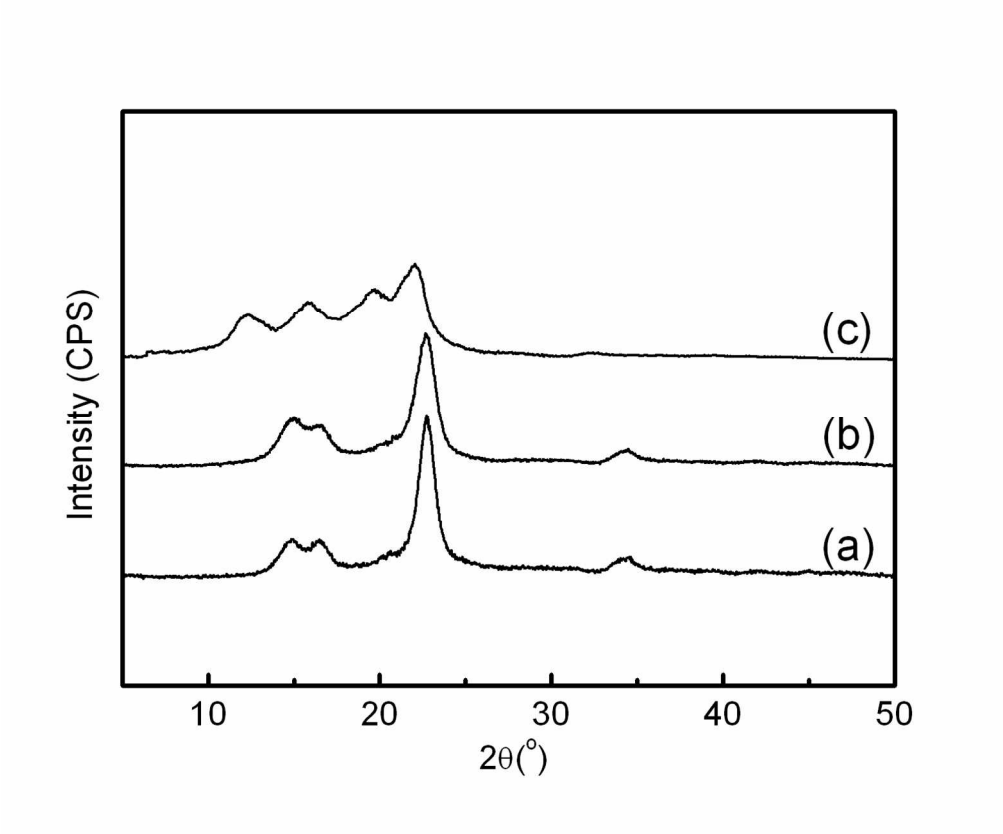

Figure 3 WAXD 2θ distributions of (a) original cellulose, (b) regenerated cellulose, (c) cellulose-g-PLA
262x219mm (150 x 150 DPI)

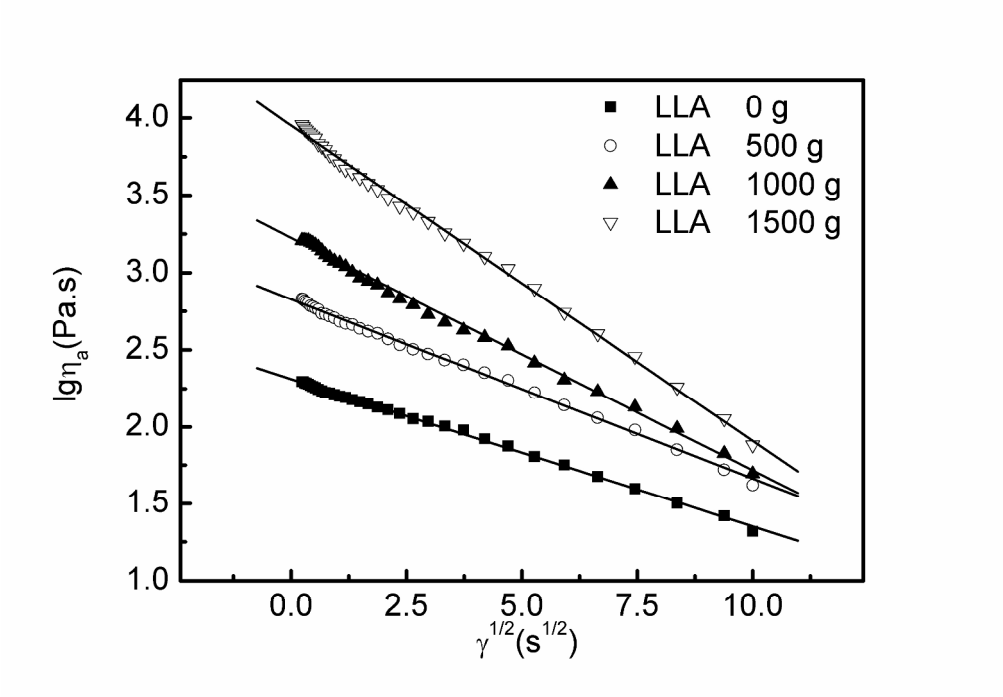

Figure 4 lgηa versus γ1/2 for cellulose/[AMIM]Cl and cellulose-g-PLA/[AMIM]Cl blends
289x202mm (300 x 300 DPI)

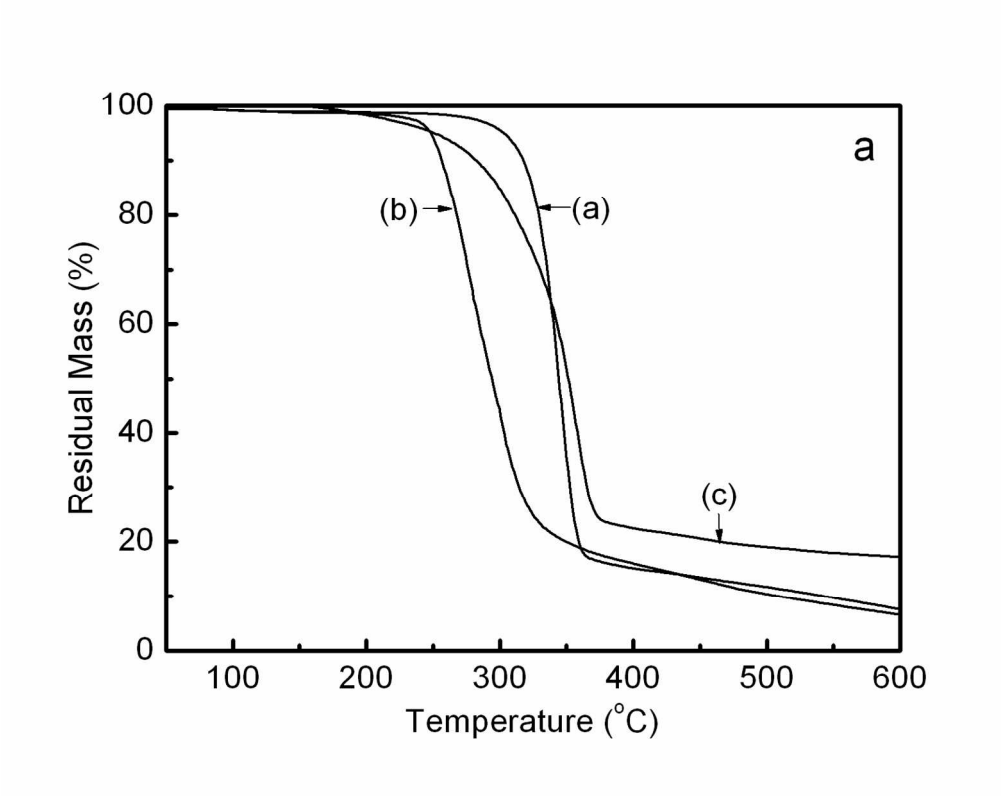

Figure 5a TGA curves of (a) original cellulose, (b) regenerated cellulose fiber, (c) cellulose-g-PLA blend fiber
276x220mm (150 x 150 DPI)

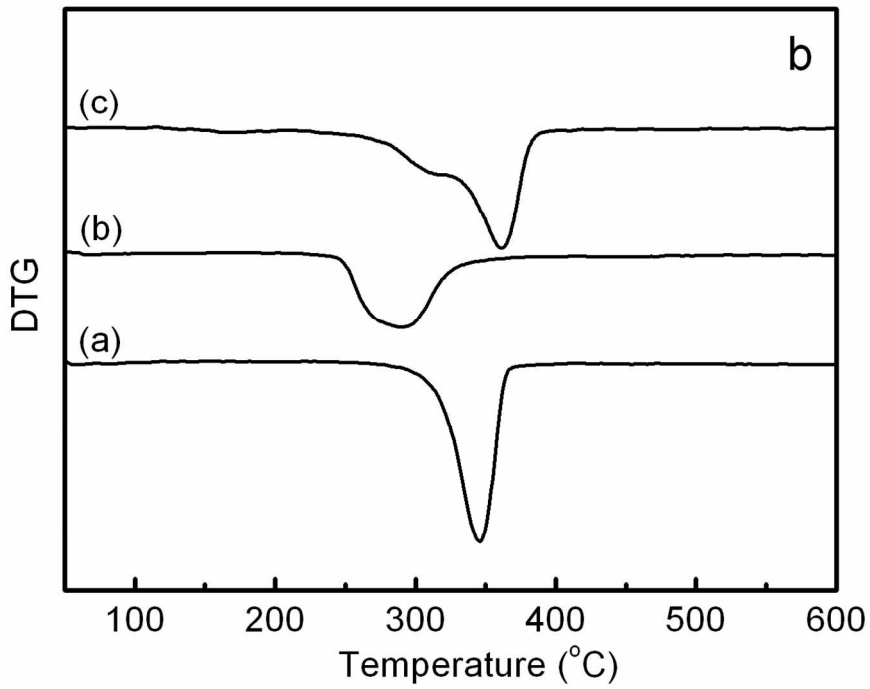

Figure 5b DTG curves of (a) original cellulose, (b) regenerated cellulose fiber, (c) cellulose-g-PLA blend fiber
250x213mm (150 x 150 DPI)

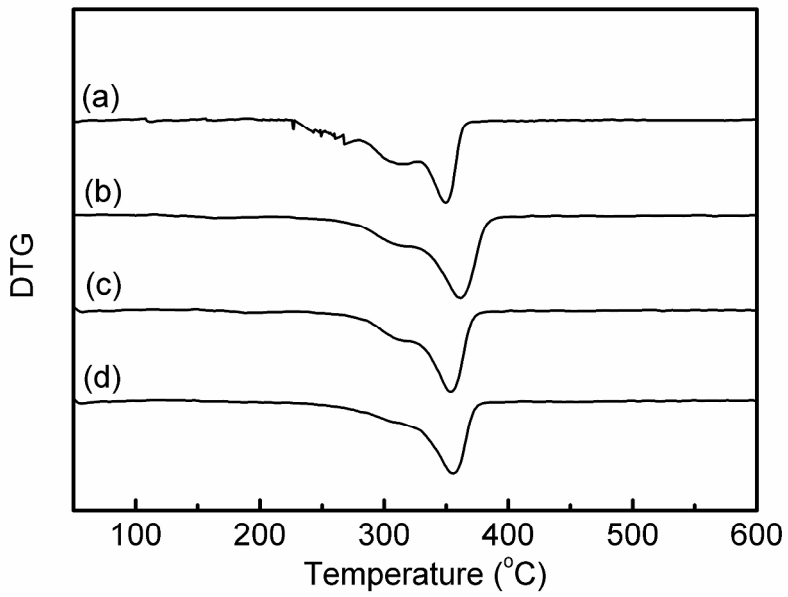

Figure 6 DTG curves of cellulose-g-PLA blend fiber prepared at different screw rotation speed (a) 25 rpm, (b) 50 rpm, (c) 75 rpm, (d) 100 rpm
289x202mm (300 x 300 DPI)

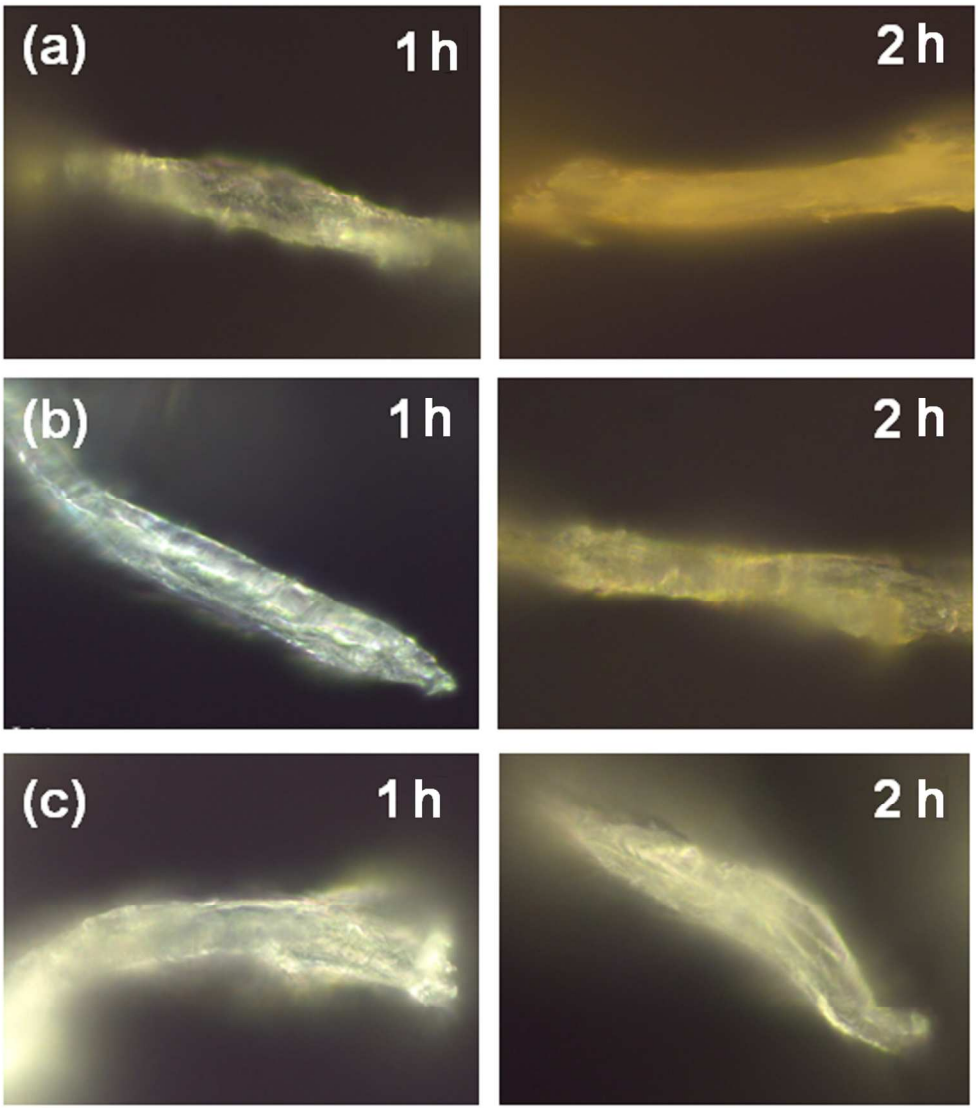

Figure 7 The microscope pictures of (a) regenerated cellulose fiber prepared by batch reactor, (b) regenerated cellulose fiber prepared by twin-screw extruder, (c) cellulose-g-PLA blend fiber after ultraviolet irradiation at 80 oC for 1-2 h
312x347mm (96 x 96 DPI)

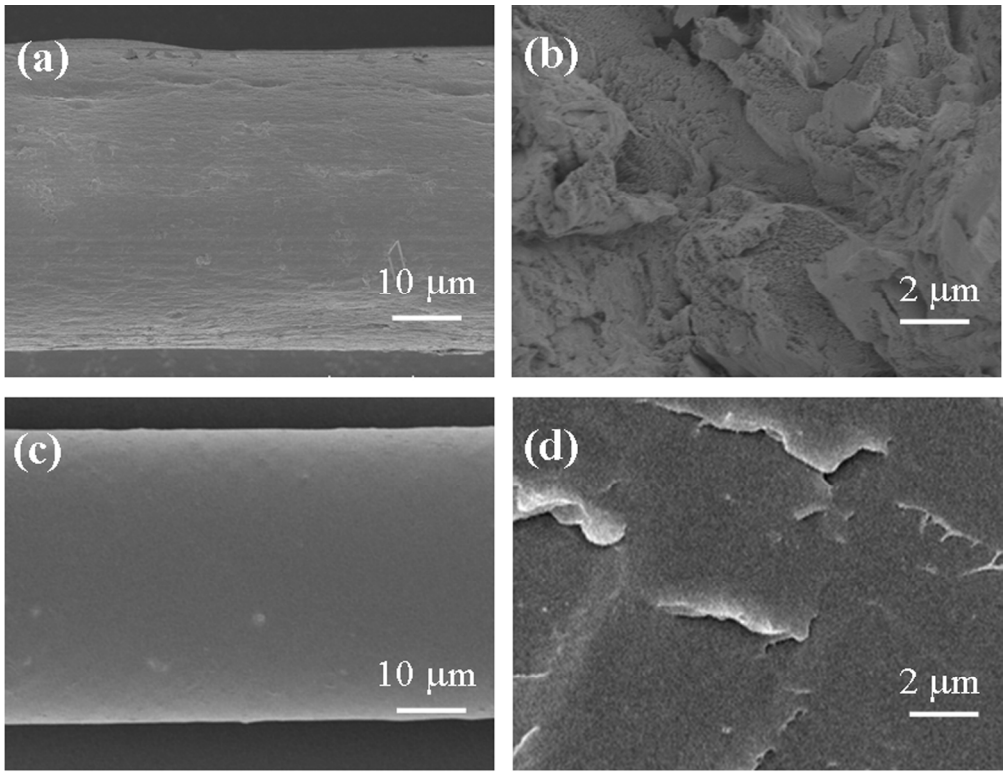

Figure 8 SEM morphologies of regenerated cellulose fiber: (a) surface, (b) cross section and cellulose-g-PLA blend fiber: (c) surface, (d) cross section
217x166mm (300 x 300 DPI)